Science of the Total Environment 915 (2024) 170024

Contents lists available at ScienceDirect

Science of the Total Environment

journal homepage: www.elsevier.com/locate/scitotenv

Impacts of projected changes in sea surface temperature on ozone pollution in China toward carbon neutrality

Jiangtao Zhu [a], Yang Yang [a,*], Hailong Wang [b], Jiyuan Gao [a], Chao Liu [a], Pinya Wang [a], Hong Liao [a]

[a] Joint International Research Laboratory of Climate and Environment Change, Jiangsu Key Laboratory of Atmospheric Environment Monitoring and Pollution Control, Jiangsu Collaborative Innovation Center of Atmospheric Environment and Equipment Technology, School of Environmental Science and Engineering, Nanjing University of Information Science and Technology, Nanjing, Jiangsu, China

[b] Atmospheric Sciences and Global Change Division, Pacific Northwest National Laboratory, Richland, WA, USA

HIGHLIGHTS

- Changes in O_3 concentrations in China due to SST changes over various oceans in the carbon neutral future are investigated.
- Under carbon neutrality, the North Pacific Ocean cooling will decrease O_3 concentrations in eastern China by reducing chemical production.
- Cooling in the Southern Hemisphere oceans weakens the vertical transport, causing a decline of O_3 in eastern China.

GRAPHICAL ABSTRACT

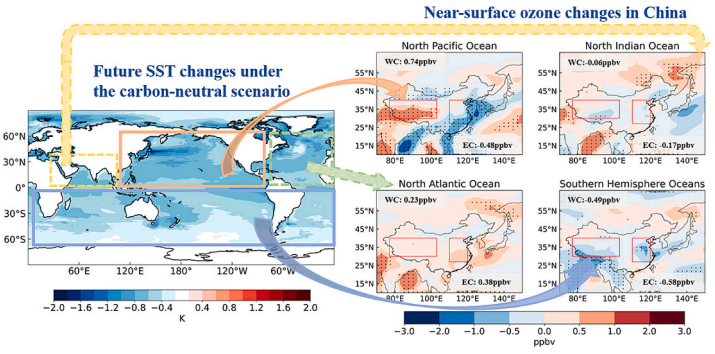

ARTICLE INFO

Editor: Hai Guo

Keywords:
Near-surface ozone
Sea surface temperature
Carbon-neutral scenario
Climate change

ABSTRACT

The global sea surface temperatures (SSTs) are expected to change diversely in the future under different climate scenarios, which will affect the near-surface ozone (O_3) distribution and concentration by influencing meteorological states and large-scale atmospheric circulation. Many countries have planned to reach carbon neutrality by the mid-21st century. In this study, the impacts of global and regional SST changes on near-surface O_3 concentrations in China in the middle of the 21st century under the carbon-neutral scenario (Shared Socioeconomic Pathway 1–1.9), compared with the high-emission scenario (Shared Socioeconomic Pathway 5–8.5), and possible physical and chemical mechanisms are investigated using the Community Earth System Model version 1 (CESM1). Under future climate change, the changes in SSTs in the carbon-neutral scenario relative to the high-emission scenario lead to a dipole change in near-surface O_3 concentrations in eastern and western China, with a significant decrease of 0.79 ppbv in the eastern China and a significant increase of 1.05 ppbv in the western China. The cooling of North Pacific Ocean under the carbon-neutral scenario causes a decrease in near-surface O_3 concentrations by 0.48 ppbv in eastern China due to the weakened chemical production and an increase by 0.74 ppbv in western China attributed to the enhanced O_3 transport from Eurasia. Cooling of Southern Hemisphere oceans leads to anomalous upward air motions over eastern China, which weaken the vertical transport of high-

* Corresponding author.
E-mail address: yang.yang@nuist.edu.cn (Y. Yang).

https://doi.org/10.1016/j.scitotenv.2024.170024
Received 23 October 2023; Received in revised form 7 January 2024; Accepted 7 January 2024
Available online 13 January 2024

elevation O_3 to the surface, resulting in a reduction in near-surface O_3 concentrations by 0.58 ppbv in eastern China. Our results suggest that future changes in SSTs in the carbon-neutral scenario will positively benefit O_3 air quality improvement in the polluted eastern China, with the North Pacific and Southern Hemisphere oceans playing important roles.

1. Introduction

Ozone (O_3) in the troposphere is a harmful air pollutant, imposing negative impacts on both human health and ecosystems (Lucas et al., 2019; Meleux et al., 2007; Monks et al., 2015). It is a strong oxidant that can cause respiratory inflammation, lower immune systems, and even result in premature aging and death in humans (Kampa and Castanas, 2008; Manisalidis et al., 2020; Pillai et al., 2005). O_3 has phytotoxic effects on plant growth and can reduce crop yield (Tai et al., 2014; Yue et al., 2017). In recent years, O_3 pollution is getting more serious in China (Gao et al., 2022; Wang et al., 2022). To address the air pollution issue, it is important to understand the physical and chemical mechanisms that lead to O_3 pollution in China.

Tropospheric O_3 is primarily produced by the photochemical reaction of volatile organic compounds (VOCs) and nitrogen oxides ($NO_x = NO + NO_2$) under the condition of sunlight (Jenkin and Clemitshaw, 2000; Kleinman, 2005; Schnell et al., 2009), which generally peaks in summer (Oltmans and Levy, 1994; Xie et al., 2017). Because O_3 is almost insoluble in water, dry deposition is the main removal process of ground-level O_3 (Fowler et al., 2008). Additionally, regional transport and mixing processes can impact near-surface O_3 concentrations, as O_3 and its precursors are often moved around on regional, intercontinental, and even hemispheric scales due to its relatively long lifetime in the troposphere (Li et al., 2023b; Monks et al., 2009; Young et al., 2013).

Meteorological conditions, such as temperature, radiation, cloudiness, and relative humidity, exert significant influences on the photochemical reactions and transport processes of O_3 (Xie et al., 2016; Yin et al., 2019). Temperature can affect O_3 production by altering photochemical reaction rates and naturally emitted O_3 precursors like plant-emitted isoprene (Guenther et al., 1993; Pusede et al., 2015; Rasmussen et al., 2012; Sillman and Samson, 1995). Radiation primarily impacts O_3 concentration by altering the photochemical reaction rate to produce O_3, whereas cloudiness typically affects O_3 through its linkage with radiation and temperature (DeCaria et al., 2005; Jasaitis et al., 2016). An increase in relative humidity can trigger the formation of hydroxyl radicals (OH) from the excited oxygen atom O(1D) of O_3 decomposition, thereby causing a decline in O_3 concentration. Numerous studies have reported a negative correlation between relative humidity and surface O_3 concentration (e.g., Gong and Liao, 2019). Atmospheric circulation also influences O_3 concentrations via transport and dispersion mechanisms (Brown-Steiner and Hess, 2011; Lin et al., 2014). Studies have found that strong westerly winds during the strong positive phase of the North Atlantic Oscillation (NAO) can transport pollutants from North America to northeastern Europe, significantly affecting surface and tropospheric O_3 concentrations over many parts of Europe (Christoudias et al., 2012). In China, significant positive correlations exist between summer O_3 concentrations and the East Asian Summer Monsoon (EASM) index, and it is suggested that cross-regional O_3 transport is the primary cause of the difference in summertime O_3 concentrations between strong and weak monsoons (Yang et al., 2014; Zhou et al., 2022). The El Niño–Southern Oscillation (ENSO) (Jiang and Li, 2022; Yang et al., 2022) and stratospheric quasi-biennial oscillation (Li et al., 2023c) are also reported to affect O_3 concentrations in China through changing large-scale circulation patterns.

Many studies have revealed that climate change could influence O_3 concentrations through perturbing meteorological conditions (Li et al., 2023a; Zanis et al., 2022). SST is an important variable for characterizing climate change (Harzallah and Sadourny, 1995), and its changes affect the energy and mass exchange between the atmosphere and the ocean (Deser et al., 2010), which can affect global climate and weather through perturbing atmospheric circulation and teleconnection patterns (Enfield and Mestas-Nuñez, 1999; Vecchi and Soden, 2007; Yoo et al., 2006). Since the industrialization, anthropogenic activities have caused global mean SST to increase (IPCC, 2021). Anthropogenic activities, especially the emission of greenhouse gases (GHGs), produced positive radiative forcing and subsequently warmed the climate system (Trenberth et al., 2014; Wijffels et al., 2016; Cheng et al., 2022). More than 90 % of the Earth's energy imbalance is stored in the oceans, leading to an increase in ocean heat content (Hansen et al., 2011).

SST anomalies (SSTAs) in different ocean basins have important influences on climate over China (Hu, 1997; Hu et al., 2011; Liu and Duan, 2018; Rong et al., 2010; Zhang et al., 2022; Jiang et al., 2014). ENSO, the largest natural variability of SST in the equatorial Pacific Ocean, can influence China's climate through changing the Hadley circulation and Rossby heat transport (Chen et al., 2012). The warming of the tropical Indian Ocean in the late 1970s caused anomalous sinking currents in the South China Sea, exacerbating the interannual warming effect on Asian summer climate (Sun et al., 2019). Ham et al. (2013) found that cooling of the tropical Atlantic SST contributes to Mid-Pacific warming and negative Atlantic Niño contributes to an enhanced East Pacific warming, thereby influencing East Asian climate by affecting the variability of ENSO events.

Some studies have demonstrated that climate responses to the SSTAs in various oceans subsequently induce modifications in spatial distribution of tropospheric O_3 by influencing local meteorological states, long-distance transport, as well as the stratosphere-troposphere exchange (Fu and Tian, 2019). For instance, Liu et al. (2005) found that El Niño events affect the transport of O_3 in the tropical and subtropical eastern Pacific in winter. Shen and Mickley (2017) observed that the occurrence of El Niño had an impact on the moisture transport, resulting in varying levels of surface O_3 during summer in the United States. Yang et al. (2022) pointed out that weakened southerly winds causes O_3 convergence during El Niño years, leading to increases in summertime O_3 concentrations in southern China. Yi et al. (2017) observed that warming of specific oceans in the Northern Hemisphere, e.g., North Pacific Ocean and North Atlantic Ocean, altered the summer surface O_3 distribution from the upwind (west of the ocean basin) to downwind (east of the ocean basin) areas.

The long-term goal of the Paris Agreement is to limit the increase in global average temperature to <2 °C above pre-industrial level and strive to limit it to <1.5 °C (Schleussner et al., 2016; Gao et al., 2017). In order to achieve the 1.5 °C target, most of the world's countries are required to be carbon neutral (CO_2 emissions balanced by removals) by the mid-21st century. The Shared Socioeconomic Pathway 1–1.9 (SSP119) is a future sustainable development scenario that is most likely to achieve the 1.5 °C target under the Paris Agreement and carbon neutrality in the mid-21st century, while the Shared Socioeconomic Pathway 5–8.5 (SSP585) is a high fossil fuel emissions scenario (Su et al., 2021; Meinshausen et al., 2020). To our knowledge, few studies have examined the effects of projected SSTAs over different oceans on future O_3 pollution in China. In this study the impacts of the projected SSTAs over individual oceans, including North Pacific, North Atlantic, North Indian Ocean, and Southern Hemisphere oceans, toward carbon neutrality on future surface O_3 concentrations during the warm season (May–October) in China are investigated based on global chemistry model simulations. In Sect. 2, we describe the model details and numerical experiments. The impacts of projected SSTAs on surface O_3 in China and the possible mechanisms are explored in Sect. 3. Conclusions

and discussion are given in Sect. 4.

2. Methods

2.1. Model description and configuration

To explore the effect of changes in SST on O_3, the Community Earth System Model version 1 (CESM1) is configured to use the Community Atmosphere Model version 4.0 (CAM4), with a horizontal resolution of 1.9°latitude × 2.5°longitude and 26 vertical layers. The chemical mechanism coupled in the CAM4 is primarily based on the Model for ozone and Related chemical Tracers, version 4 (MOZART-4), which resolves 85 gas-phase species and 196 gas-phase reactions (Emmons et al., 2010).

In this study, the ocean components are prescribed with climatological SST distributions. The projected multi-model mean SST data for both SSP119 and SSP585 scenarios from the Scenario Model Intercomparison Project (ScenarioMIP) under CMIP6 are used to drive the model. Totally 8 global climate models (GCMs) are adopted, including CAMS-CSM1–0, CanESM5, EC-Earth3-Veg-LR, EC-Earth3-Veg, FGOALS-g3, GFDL-ESM4, MIROC6, and MRI-ESM2–0. Anthropogenic emissions of chemical species and biomass burning emissions are also provided by CMIP6 (Hoesly et al., 2018; van Marle et al., 2017). Biogenic emissions are prescribed as in Tilmes et al. (2016). All emissions, including anthropogenic emissions, biomass burning emissions and natural emissions, are fixed at the year of 2010 to distinguish the impacts of SST variations on O_3 distributions.

2.2. Experimental design

In this work, a total of six sensitivity experiments are performed to quantify the future changes in SST on O_3 between the carbon-neutral scenario (SSP119) and high-emission scenario (SSP585) by 2050 and isolate the roles of SSTAs over the North Pacific, North Atlantic, North Indian Ocean, and Southern Hemisphere oceans. The ocean division in the Northern Hemisphere follows Yi et al. (2017) and we also include the Southern Hemisphere oceans in this study. All experiments are driven by the future monthly mean SST around 2050 (average over 2045–2054). All simulations are run for 30 years with the first 15 years used for model spin-up, including atmospheric adjustment to the SST changes, and the averages of the last 15 years used for analyses. The six sensitivity experiments are as follows:

(1) ALL585: future SSTs under the SSP585 scenario are used to drive the model.

(2) ALL119: future SSTs under the SSP119 scenario are used to drive the model.

(3–6) NP/NA/NI/SO119: Same as ALL585, but SSTs in individual oceans, i.e., North Pacific Ocean (NP), North Atlantic Ocean (NA), North Indian Ocean (NI), and Southern Hemisphere Oceans (SO) are replaced with those under SSP119 scenario.

The changes in SSTs of individual oceans are shown in Fig. S1. The differences in O_3 between ALL585 and ALL119 are attributed to the differences in global SSTs between high-emission scenario and carbon-neutral scenario. In addition, comparisons between ALL585 and NP/NA/NI/SO119 can be used to quantify the impacts of changes in SSTs over the individual oceans toward carbon neutrality on O_3 levels, relative to the high emission scenario. In this study, we focus on the O_3 concentrations during the warm season from May to October, when the O_3 pollution is the most severe in China.

The CESM1-CAM4 model has been extensively evaluated in simulating tropospheric O_3 in present-day levels. It can well reproduce the O_3 concentrations in the Northern Hemisphere (Tilmes et al., 2015). However, some studies also revealed that the model overestimated near-surface O_3 concentrations over North America and Europe (Lamarque et al., 2012; Li et al., 2023b; Phalitnonkiat et al., 2018; Val Martin et al., 2015). An additional simulation driven by global SSTs in 2010 (average over 2005–2014) is also performed and roughly compared to O_3 observations in China during 2013–2020. The results show that the near-surface O_3 concentration in eastern China (27°–40°N,110°–120°E) is well captured by the model, with the bias <10 %, while the O_3 concentration in western China (30°–40°N,77°–103°E) is overestimated by about 50 %, likely related to the high O_3 bias in the upwind regions (Fig. S2).

3. Results

3.1. Response of near-surface O_3 concentrations to SST changes

In the mid-21st century, reduced GHGs in the carbon-neutral scenario (SSP119) lead to substantial decreases in SSTs across the world (Fig. S3a), especially in the Northern Hemisphere, compared to the high-emission scenario (SSP585). The decreases in SSTs further result in increases in near-surface O_3 concentrations from 30°S to the North Pole (Fig. S3b), associated with lower water vapor abundances in a cooler climate (Zanis et al., 2022). In contrast, near-surface O_3 concentrations decline significantly in the polluted areas, including East Asia and northern part of Southeast Asia, likely related to a strong reduction in the photochemical production of O_3. The global spatial pattern of projected changes in near-surface O_3 is in accordance with previous studies (Zanis et al., 2022; IPCC, 2021). In this study, we focus on the impacts of future changes in SSTs on near-surface O_3 in China (Fig. 1). A dipole pattern with negative O_3 anomalies in eastern China and positive O_3 anomalies in western China forms in response to the global changes in SSTs under the carbon neutrality scenario, compared to the high-emission scenario in 2050 (Fig. 1). Over eastern China (27°–40°N,110°–120°E), the global decreases in SSTs lead to a regional O_3 decrease by 0.79 ppbv, while the regional O_3 concentration increases by 1.05 ppbv averaged over western China (30°–40°N,77°–103°E), with the maximum O_3 changes in the range of 1–2 ppbv in China.

The future changes in O_3 concentrations over China driven by the SST changes can be decomposed into the contributions from changing SSTs of different oceans. Fig. 2 shows changes in near-surface O_3 concentrations in China averaged over May–October due to the SST changes in four oceanic regions, including North Pacific, North Indian Ocean,

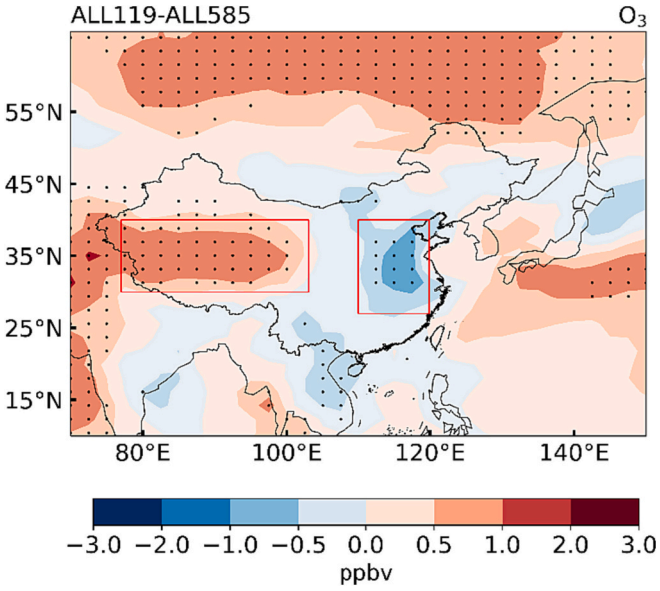

Fig. 1. Changes in near-surface O_3 concentrations (ppbv) averaged over May–October between ALL119 and ALL585 (ALL119 – ALL585). The two regions of interest (i.e., western China: 30°–40°N, 77°–103°E and eastern China: 27°–40°N,110°–120°E) are marked with red box. The stippled areas indicate statistical significance with 90 % confidence from a two-tailed *t*-test.

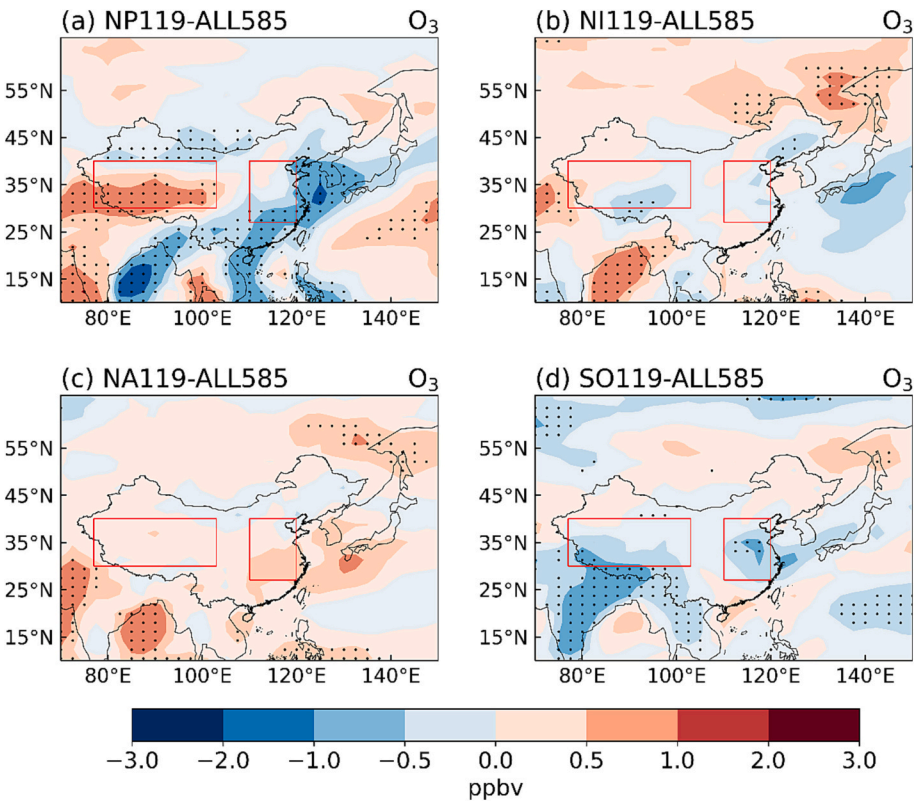

Fig. 2. Changes in surface O_3 concentrations (ppbv) averaged over May–October between (a) NP119 and ALL585, (b) NI119 and ALL585, (c) NA119 and ALL585, and (d) SO119 and ALL585. The stippled areas indicate statistical significance with 90 % confidence from a two-tailed t-test.

North Atlantic, and Southern Hemisphere oceans, between the carbon-neutral and high-emission scenarios in 2050. The decreases in SSTs over the North Pacific Ocean cause significant decreases in near-surface O_3 concentrations in the south of eastern China and significant increases in western China (Fig. 2a). Averaged over the two regions in China, the cooler SSTs over the North Pacific Ocean toward carbon neutrality contribute to the O_3 changes by −0.48 ppbv in eastern China and 0.74 ppbv in western China, compared to the high-emission scenario, explaining 30 % and 49 % of the O_3 changes driven by the global SST changes. The impacts of SST changes in North Indian Ocean and North Atlantic Ocean on near-surface O_3 levels in China are not pronounced, as depicted in Fig. 2b and c. Additionally, SSTs changes in the Southern Hemisphere oceans also cause significant decreases in near-surface O_3 concentrations in central area of eastern China, with a regionally averaged change of −0.58 ppbv in eastern China (Fig. 2d). The cooling of SSTs in the Southern Hemisphere oceans explains 36 % of the O_3 change driven by the global SST changes, which is the dominant factor causing the decrease in near-surface O_3 concentrations in eastern China.

The sum of the responses of near-surface O_3 concentrations in China to SST changes over the four individual oceanic regions shows a similar spatial pattern as their response to global SST changes (Fig. S4), with decreases in O_3 concentrations over eastern China and increases in western China. Note that, the magnitudes of changes are slightly different between the sum of responses to SST changes over individual oceans and the response to the global SST changes. It is because the responses of meteorological parameters to SSTs are likely non-linear and the O_3 chemistry does not respond to the changes in meteorological parameters linearly. However, the similar spatial patterns indicate that the effects of global SST cooling under the carbon neutral-scenario on near-surface O_3 concentrations in China can be decomposed into contributions from broad regional SST forcings, which is consistent with previous studies (Fan et al., 2016; Seager and Henderson, 2016).

The results above suggest that the decline in near-surface O_3 levels in eastern China due to the global ocean cooling under the carbon-neutral scenario compared to the high-emission scenario in 2050 are primarily attributed to the decreases in SSTs over the North Pacific Ocean and Southern Hemisphere oceans. The rises in near-surface O_3 levels in western China are primarily attributed to the decreases in SSTs over the North Pacific Ocean.

3.2. *Possible underlying mechanisms for the responses of O_3 in China*

A comprehensive understanding of the potential underlying mechanisms that can explain the responses of O_3 in China to changes in SSTs in different future climate scenarios is crucial to develop effective strategies to mitigate the O_3 pollution in China. In this section, we aim to examine the possible mechanisms of the impacts of SST changes over individual ocean basins, especially over the North Pacific Ocean and Southern Hemisphere oceans, on near-surface O_3 levels in China, by gaining more insight into the impact of SST changes on local meteorological conditions and large-scale atmospheric circulations.

The simulated changes in the net production rate of O_3 at the surface during May–October in 2050 due to the SST decreases in different oceans under the carbon-neutral versus the high-emission scenarios are illustrated in Fig. 3. The decreases in SSTs in the North Pacific Ocean cause significant decreases in O_3 production in the south of eastern China and coastal areas and increases in central China (Fig. 3a), which are in line with the decreases in O_3 concentrations in eastern China (Fig. 2a). However, the decreases in chemical production cannot explain the increases in O_3 concentrations in western China. The decreases in SSTs in the Southern Hemisphere oceans enhance the net O_3 production in eastern China (Fig. 3d), which is opposite to the changes in O_3 concentrations (Fig. 2d). Net O_3 productions in eastern and western China are not noticeably affected by SST changes in the North Indian Ocean or North Atlantic Ocean (Fig. 3b and c).

As the precursor emissions are kept the same in all experiments, the

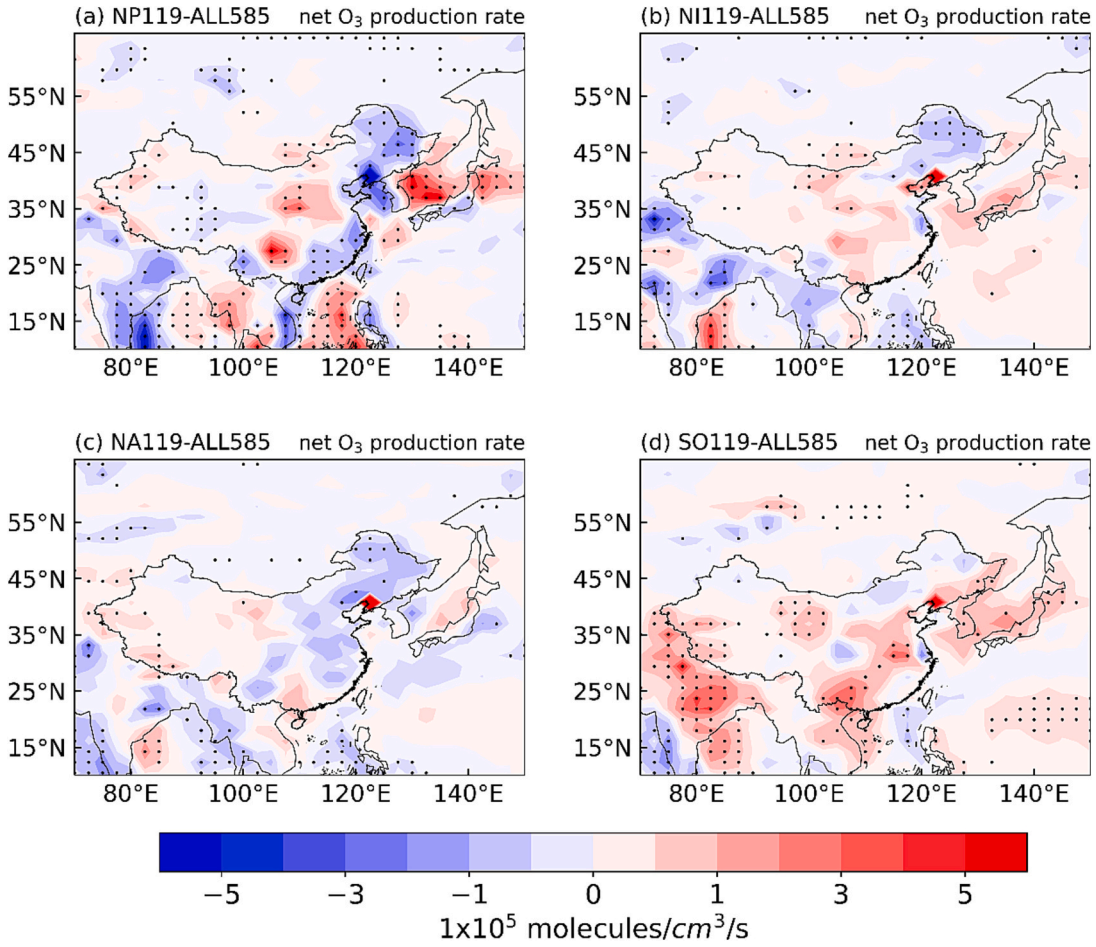

Fig. 3. Changes in the surface net O_3 production rate (production – loss) averaged over May–October (1×10^5 molecules cm^{-3} s^{-1}) between (a) NP119 and ALL585, (b) NI119 and ALL585, (c) NA119 and ALL585, and (d) SO119 and ALL585. The stippled areas indicate statistical significance with 90 % confidence from a two-tailed t-test.

changes in net O_3 production are primarily attributed to meteorological changes. Figs. 4–7 shows respectively the responses of surface air temperature, low cloud fraction, net solar flux at the surface, and surface relative humidity to SST changes between the carbon-neutral and high-emission scenarios over May–October in 2050. The ocean cooling in the North Pacific leads to a decrease in surface air temperature by 0.4–0.8 K

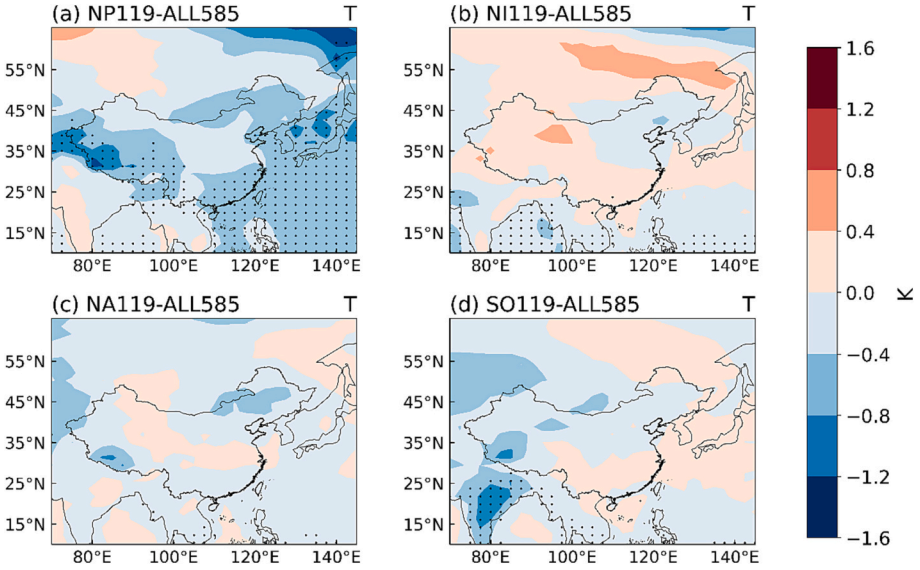

Fig. 4. Changes in surface air temperature (K) averaged over May–October between (a) NP119 and ALL585, (b) NI119 and ALL585, (c) NA119 and ALL585, and (d) SO119 and ALL585. The stippled areas indicate statistical significance with 90 % confidence from a two-tailed t-test.

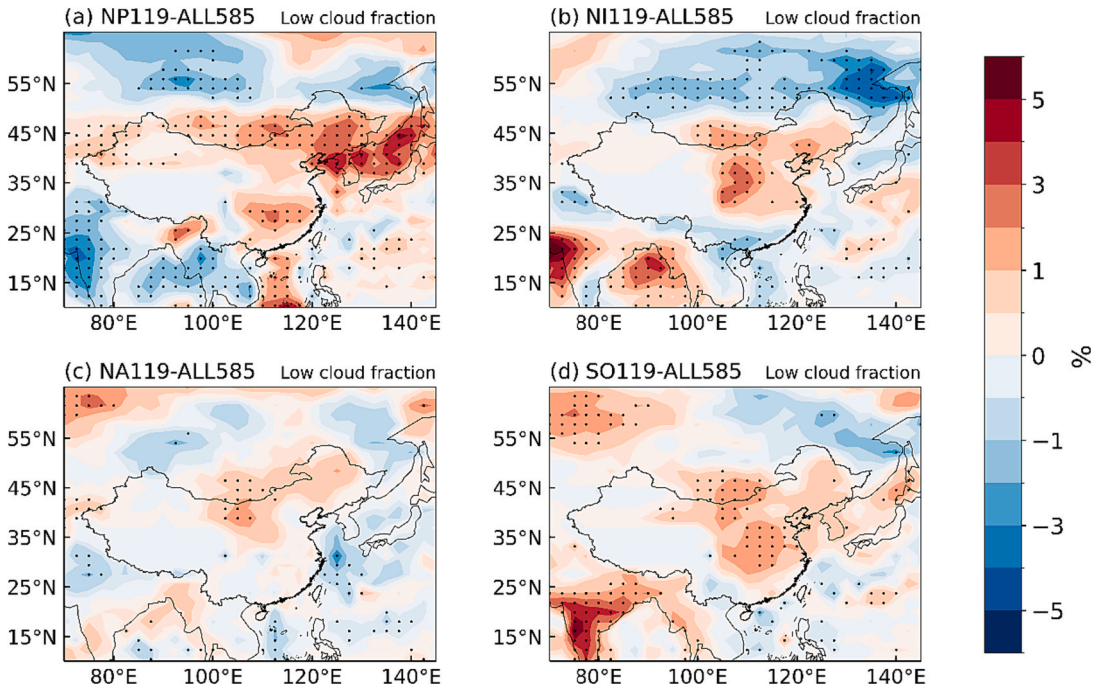

Fig. 5. Changes in low cloud fraction (%) averaged over May–October between (a) NP119 and ALL585, (b) NI119 and ALL585, (c) NA119 and ALL585, and (d) SO119 and ALL585. The stippled areas indicate statistical significance with 90 % confidence from a two-tailed t-test.

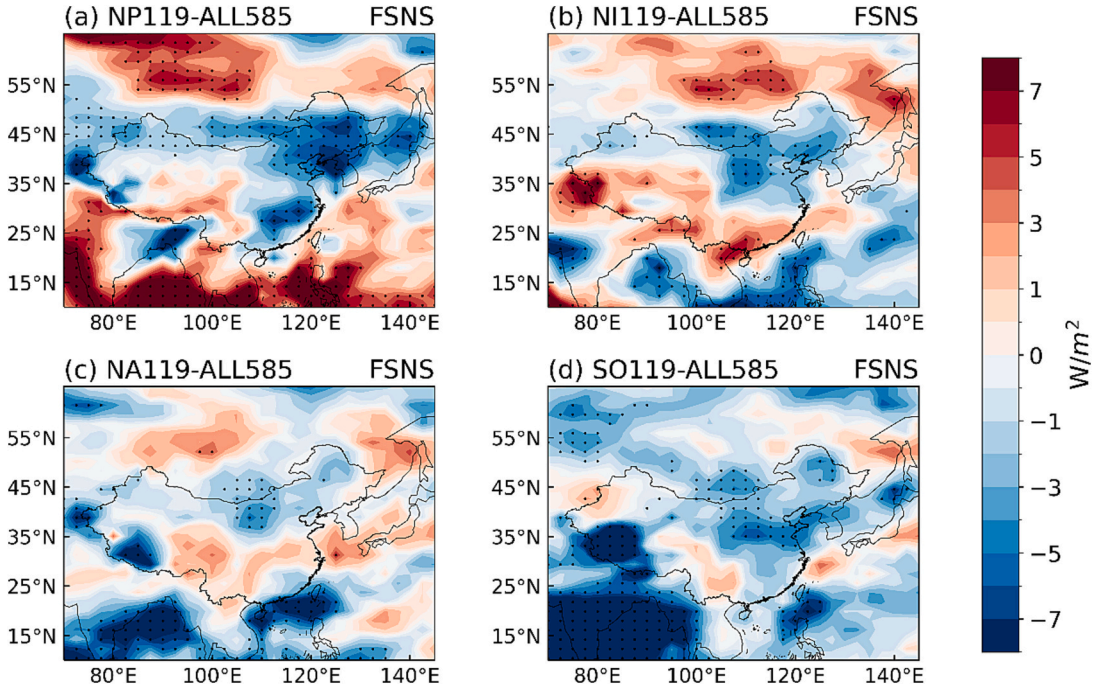

Fig. 6. Changes in net solar flux at the surface (FSNS, W m^{-2}) averaged over May–October between (a) NP119 and ALL585, (b) NI119 and ALL585, (c) NA119 and ALL585, and (d) SO119 and ALL585. The stippled areas indicate statistical significance with 90 % confidence from a two-tailed t-test.

over southern China and western China (Fig. 4a). The associated decrease in convection increases the low cloud fraction (Fig. 5a), which results in more reflection of solar radiation back to the space and a reduction in net solar flux at the surface (Fig. 6a). The cooler air, more low-level clouds, less solar radiation, and higher relative humidity (Fig. 7a) in response to the decreases in SSTs over the North Pacific Ocean cause the decreases in O_3 production in the south of eastern China. Although the low-level cloud increases (Fig. 5d), solar radiation decrease (Fig. 6d), and relative humidity increases (Fig. 7d) in response to the decreases in SSTs over the Southern Hemisphere oceans, the O_3 production increases (Fig. 3d), which is related to the changes in O_3 precursor distributions. The colder SSTs of the Southern Hemisphere oceans lead to an increase in the O_3 precursors (NO_x and VOCs) over many areas of eastern China (Fig. S5). Due to the anomalous easterly winds over eastern China associated with the anomalous low over south of China (Fig. S6), the zonal component of the prevailing southwesterly

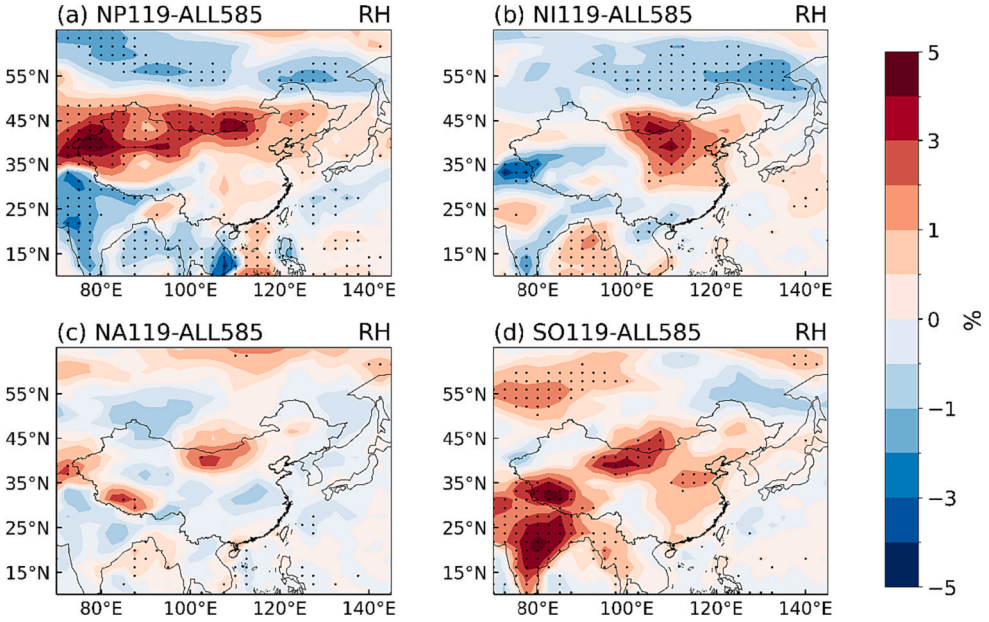

Fig. 7. Changes in surface relative humidity (RH, %) averaged over May–October between (a) NP119 and ALL585, (b) NI119 and ALL585, (c) NA119 and ALL585, and (d) SO119 and ALL585. The stippled areas indicate statistical significance with 90 % confidence from a two-tailed t-test.

winds is weakened, which is not conducive to the diffusion of O_3 precursor to the oceans, leading to the increases in O_3 precursor concentrations and thus the increase in the net O_3 production.

SST anomalies can influence atmospheric circulation patterns, which further affects the horizontal and vertical transport of O_3. The increases in near-surface O_3 concentrations over western China (e.g., the Tibetan Plateau) caused by the decreases in SSTs in North Pacific Ocean (Fig. 2a), which cannot be explained by local chemical processes, are probably related to changes in long-range transport of O_3. Studies have shown that near-surface O_3 anomalies over the Tibetan Plateau are less influenced by the local production but more influenced by the stratospheric intrusion and long-range transport (Ding and Wang, 2006; T.

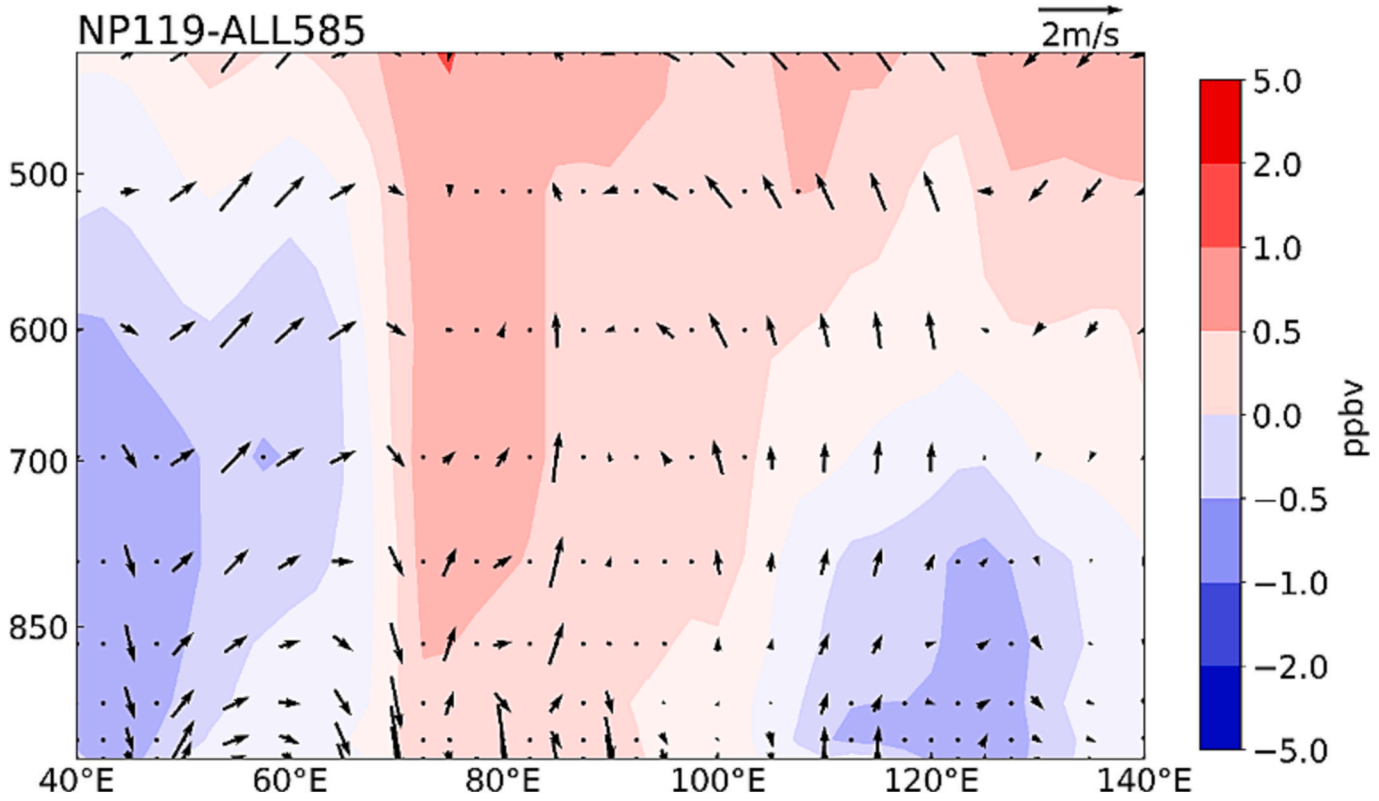

Fig. 8. Pressure-longitude cross sections averaged over 30°–40°N for differences in O_3 concentrations (ppbv, contours), zonal winds (m s^{-1}, vectors) and pressure velocity (Pa s^{-1}, vectors) between NP119 and ALL585 (NP119 – ALL585) averaged over May–October. Note that the pressure velocity is multiplied by a factor of −200.The stippled areas indicate statistical significance with 90 % confidence from a two-tailed t-test.

Wang et al., 2006). According to Li et al. (2014), emissions from Eurasia except China led to an increase of 10 to 15 ppbv in the surface O_3 mixing ratio during spring and summer over western China due to long-range transport. As shown in Fig. 8, the decreases in SSTs in the North Pacific lead to anomalous westerly winds at 40–80°E, averaged over 30–40°N, which enhance the long-range transport of O_3 from upwind source regions of Eurasia and thus increase O_3 levels in western China. This can be confirmed by the enhanced O_3 flux over western China shown in Fig. S7.

The decreases in O_3 over eastern China due to the decreases in SSTs over the Southern Hemisphere oceans are attributed to the changes in large-scale atmospheric circulation patterns. As shown in Fig. 9, accompanied by the ocean surface cooling, the atmospheric heating rate decreases significantly over the Southern Hemisphere oceans, especially over the areas near 10°S. This is associated with the dampened convective activity and the decreases in evaporated water vapor that otherwise carries a large amount of latent heat. The atmospheric cooling weakens deep convection in the south of the equator and induces anomalous upward motions in the north of the equator and 15°–40°N. The anomalous upward motions weaken the downward transport of O_3 from middle and upper troposphere, causing the decreases in O_3 concentrations in eastern China. Although the colder SSTs of the Southern Hemisphere oceans lead to an increase in the O_3 precursors and enhance O_3 production mentioned above, this effect tends to be weaker than the decrease in downward transport of O_3 from middle and upper troposphere associated with anomalous vertical motions. The combined influences cause the decrease in near-surface O_3 concentrations in eastern China in response to the decreases in SSTs over the Southern Hemisphere oceans.

4. Conclusion and discussions

This study investigates the impacts of projected SST changes on future near-surface O_3 pollution during the warm season in China under the carbon-neutral scenario SSP119 relative to the high fossil fuel emission scenario SSP585, when many countries of the world achieve carbon neutrality in the middle of the 21st century, based on sensitivity experiments using the CESM1 model. With fixed emissions at present-day levels, the responses of near-surface O_3 concentrations in China to CMIP6 projected SST changes in various ocean basins, including the North Pacific, North Atlantic, North Indian Ocean, and Southern Hemisphere oceans, are investigated. The results show that the future global ocean surface cooling under the carbon-neutral scenario SSP119 leads to dipole changes in China's near-surface O_3 concentrations during May–October, with an average decrease of 0.79 ppbv in eastern China and an increase of 1.05 ppbv in western China, compared to the high-emission scenario SSP585 in 2050.

The future changes in O_3 concentrations over China driven by the global SST changes can be further decomposed into the contributions of SST changes over individual ocean basins. Compared to SSP585, the SSP119 cooling of North Pacific Ocean leads to the changes in near-surface O_3 concentrations by −0.48 ppbv in eastern China and 0.74 ppbv in western China. The decrease in O_3 level in eastern China is due to the weakened chemical productions of O_3 related to the cooler air, more low-level clouds, less solar radiation at the surface, and higher relative humidity in response to the decreases in SSTs over the North Pacific Ocean under SSP119, compared to SSP585. The increase in near-surface O_3 concentrations in western China is attributed to changes in atmospheric circulation with anomalous westerly winds that increase the O_3 transport from Eurasia to western China. The cooling of the Southern Hemisphere oceans also contributes to a 0.58 ppbv decrease in O_3 concentration in eastern China by triggering an anomalous upward motion and weakening the downward transport of O_3 from middle and upper troposphere.

In general, changes in SST in any ocean basin lead to changes in convection over the oceans, which further affects atmospheric

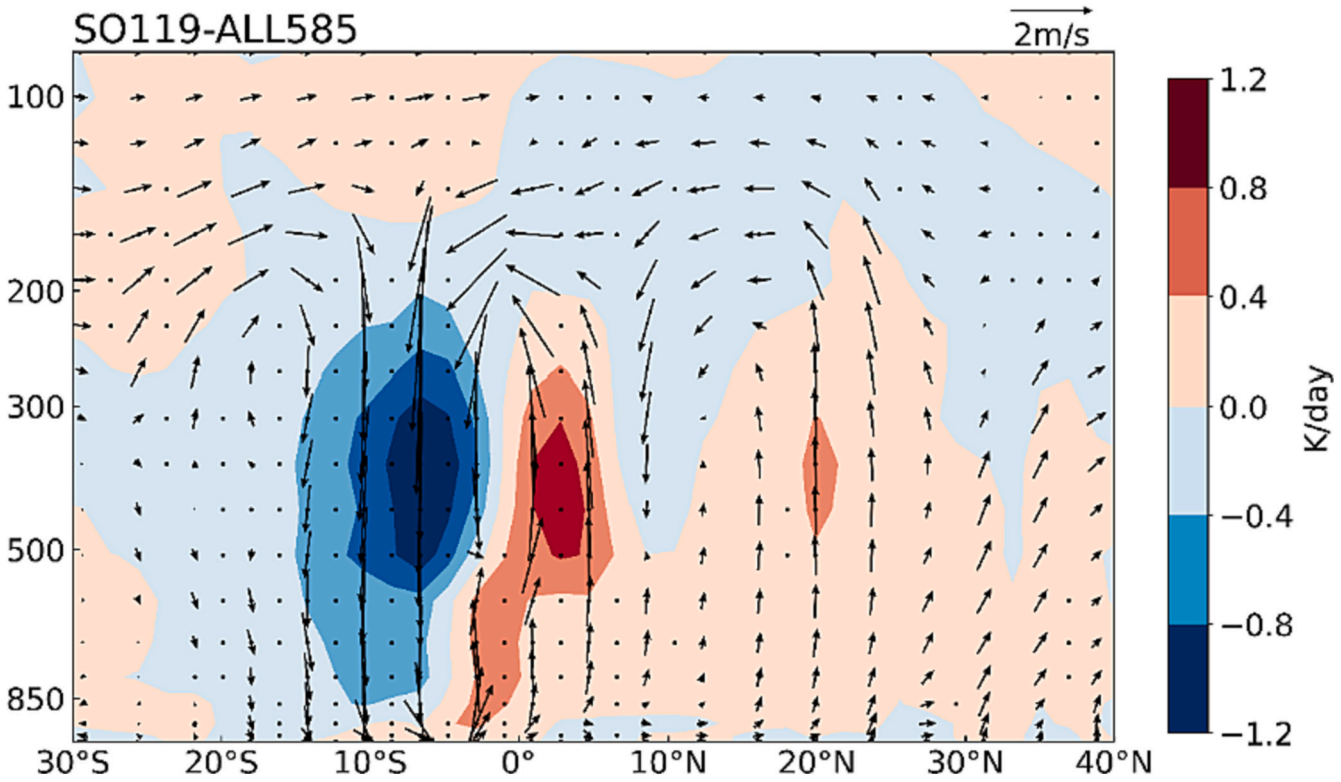

Fig. 9. Pressure-latitude cross sections averaged over 110°–120°E for differences in atmospheric heating rate (K day^{-1}, contours), meridional winds (m s^{-1}, vectors) and pressure velocity (Pa s^{-1}, vectors) between SO119 and ALL585 (SO119 – ALL585) averaged over May–October. Note that the pressure velocity is multiplied by a factor of −200. The stippled areas indicate statistical significance with 90 % confidence from a two-tailed t-test.

circulation, temperature, precipitation, cloudiness and radiation. Warm SST heats the surrounding air and form a low pressure, which triggers vertical upward motions and convection of air currents and further large-scale subsidence in the neighboring regions through the modulation of large-scale circulation patterns (Ueda et al., 2015; Yi et al., 2017). On the contrary, the cold SST causes the air to sink and forms a high pressure, which triggers large-scale upward motions in the nearby region. As shown in Fig. S6, the cold SSTs in the North Pacific Ocean lead to the emergence of high-pressure anticyclones at the sea surface and trigger updraft motions in the neighboring eastern China (110°E-120°E) (Fig. 8), which is conducive to the increase in cloudiness (Fig. 5a), decrease in radiation (Fig. 6a) and temperature (Fig. 4a). Cold SSTs in the Southern Hemisphere oceans also lead to a subsidence motion near 10°S (Fig. 9), weakening the Hadley circulation and triggering an anomalous upward motion over 15°-40°N, which further cause the increase in cloudiness (Fig. 5d), decrease in radiation (Fig. 6d) and increase in relative humidity (Fig. 7d).

By comparing the impacts of SST changes between SSP119 and SSP585 in different ocean basins on future O_3 pollution over China in the middle of the 21st century, this study provides insights into the mitigation of O_3 pollution in China. The spatial pattern of O_3 changes in China in response to global SST changes is generally consistent with previous studies (Li et al., 2023a; Zanis et al., 2022). However, the present study has some limitations that need to be further investigated. For example, the fixed SST-driven experiments only considered the oceanic impacts on the atmosphere, without considering the ocean-atmosphere interactions. The modeled near-surface O_3 concentrations are underestimated over the North China Plain and Yangtze River Delta in eastern China and overestimated in western China compared to observations, which may be related to uncertainties in precursor emissions or physical and chemical parameterizations in the model. This study focuses on the impacts of SST changes by performing simulations with fixed precursor emissions at present-day levels; however, future emissions under different scenarios are different from current present-day levels, which warrants further studies to assess the relative roles of changes in emissions versus climate in the future. In this study we only focus the O_3 pollution in China and the responses in O_3 concentrations in other countries of the world deserve further analysis in future studies.

CRediT authorship contribution statement

Jiangtao Zhu: Writing – original draft, Formal analysis. **Yang Yang:** Writing – review & editing, Supervision, Methodology, Conceptualization. **Hailong Wang:** Writing – review & editing. **Jiyuan Gao:** Methodology. **Chao Liu:** Methodology. **Pinya Wang:** Writing – review & editing. **Hong Liao:** Writing – review & editing.

Declaration of competing interest

The authors declare that they have no known competing financial interests or personal relationships that could have appeared to influence the work reported in this paper.

Data availability

The CESM is maintained by NCAR and is provided freely to the community. The multi-model future simulations of the Coupled Model Intercomparison Project Phase 6 (CMIP6) are from https://esgf-node.llnl.gov/search/cmip6/ (last access: October 2023). O_3 observations over China can be obtained from the China National Environmental Monitoring Centre (http://www.cnemc.cn, last access: October 2023). The modeling results are made available at doi:https://doi.org/10.5281/zenodo.8412654 (Yang, 2023).

Acknowledgments

This study was supported by the National Natural Science Foundation of China (grants 42293320 and 42105166), the National Key Research and Development Program of China (grant 2020YFA0607803), Jiangsu Science Fund for Distinguished Young Scholars (grant BK20211541), and the Jiangsu Science Fund for Carbon Neutrality (grant BK20220031). HW acknowledges the support by the U.S. Department of Energy (DOE), Office of Science, Office of Biological and Environmental Research (BER), as part of the Earth and Environmental System Modeling program. The Pacific Northwest National Laboratory (PNNL) is operated for DOE by the Battelle Memorial Institute under contract DE-AC05-76RLO1830.

Appendix A. Supplementary data

Supplementary data to this article can be found online at https://doi.org/10.1016/j.scitotenv.2024.170024.

References

Brown-Steiner, B., Hess, P., 2011. Asian influence on surface ozone in the United States: a comparison of chemistry, seasonality, and transport mechanisms. J. Geophys. Res. 116 https://doi.org/10.1029/2011JD015846.

Chen, Y., Zhao, Y., Feng, J., Wang, F., 2012. ENSO cycle and climate anomaly in China. Chin. J. Oceanol. Limnol. 30, 985–1000. https://doi.org/10.1007/s00343-012-1245-1.

Cheng, L., Abraham, J., Trenberth, K.E., Fasullo, J., Boyer, T., Mann, M.E., Zhu, J., Wang, F., Locarnini, R., Li, Y., Zhang, B., Tan, Z., Yu, F., Wan, L., Chen, X., Song, X., Liu, Y., Reseghetti, F., Simoncelli, S., Gouretski, V., Chen, G., Mishonov, A., Reagan, J., 2022. Another record: ocean warming continues through 2021 despite La Niña conditions. Adv. Atmos. Sci. 39, 373–385. https://doi.org/10.1007/s00376-022-1461-3.

Christoudias, T., Pozzer, A., Lelieveld, J., 2012. Influence of the North Atlantic oscillation on air pollution transport. Atmos. Chem. Phys. 12, 869–877. https://doi.org/10.5194/acp-12-869-2012.

DeCaria, A.J., Pickering, K.E., Stenchikov, G.L., Ott, L.E., 2005. Lightning-generated NOX and its impact on tropospheric ozone production: a three-dimensional modeling study of a stratosphere-troposphere experiment: radiation, aerosols and ozone (STERAO-A) thunderstorm. J. Geophys. Res. 110, D14303. https://doi.org/10.1029/2004JD005556.

Deser, C., Phillips, A.S., Alexander, M.A., 2010. Twentieth century tropical sea surface temperature trends revisited. Geophys. Res. Lett. 37, L10701. https://doi.org/10.1029/2010GL043321.

Ding, A., Wang, T., 2006. Influence of stratosphere-to-troposphere exchange on the seasonal cycle of surface ozone at mount Waliguan in western China. Geophys. Res. Lett. 33, L03803. https://doi.org/10.1029/2005GL024760.

Emmons, L.K., Walters, S., Hess, P.G., Lamarque, J.-F., Pfister, G.G., Fillmore, D., Granier, C., Guenther, A., Kinnison, D., Laepple, T., Orlando, J., Tie, X., Tyndall, G., Wiedinmyer, C., Baughcum, S.L., Kloster, S., 2010. Description and evaluation of the model for ozone and related chemical tracers, version 4 (MOZART-4). Geosci. Model Dev. 3, 43–67. https://doi.org/10.5194/gmd-3-43-2010.

Enfield, D.B., Mestas-Nuñez, A.M., 1999. Multiscale variabilities in Global Sea surface temperatures and their relationships with tropospheric climate patterns. J. Clim. 12, 2719–2733. https://doi.org/10.1175/1520-0442(1999)012<2719:MVIGSS>2.0.CO;2.

Fan, L., Shin, S.-I., Liu, Z., Liu, Q., 2016. Sensitivity of Asian Summer Monsoon precipitation to tropical sea surface temperature anomalies. Clim. Dyn. 47, 2501–2514. https://doi.org/10.1007/s00382-016-2978-x.

Fowler, D., Amann, M., Anderson, R., Ashmore, M., Cox, P., Depledge, M., Derwent, D., Grennfelt, P., Hewitt, N., Hov, O., Jenkin, M., Kelly, F., Liss, P.S., Pilling, M., Pyle, J., Slingo, J., Stevenson, D., 2008. Ground-Level Ozone in the 21st Century: Future Trends, Impacts and Policy Implications. The Royal Society, Tech. rep.

Fu, T.M., Tian, H., 2019. Climate change penalty to ozone air quality: review of current understandings and knowledge gaps. Curr. Poll. Rep. 5, 159–171. https://doi.org/10.1007/s40726-019-00115-6.

Gao, J., Yang, Y., Wang, H., Wang, P., Li, H., Li, M., Ren, L., Yue, X., Liao, H., 2022. Fast climate responses to emission reductions in aerosol and ozone precursors in China during 2013–2017. Atmos. Chem. Phys. 22, 7131–7142. https://doi.org/10.5194/acp-22-7131-2022.

Gao, Y., Gao, X., Zhang, X., 2017. The 2 °C global temperature target and the evolution of the long-term goal of addressing climate change—from the United Nations framework convention on climate change to the Paris agreement. Engineering 3, 272–278. https://doi.org/10.1016/J.ENG.2017.01.022.

Gong, C., Liao, H., 2019. A typical weather pattern for ozone pollution events in North China. Atmos. Chem. Phys. 19, 13725–13740. https://doi.org/10.5194/acp-19-13725-2019.

Guenther, A.B., Zimmerman, P.R., Harley, P.C., Monson, R.K., Fall, R., 1993. Isoprene and monoterpene emission rate variability: model evaluations and sensitivity analyses. J. Geophys. Res. 98, 12609–12617. https://doi.org/10.1029/93JD00527.

Ham, Y.G., Kug, J.S., Park, J.-Y., 2013. Two distinct roles of Atlantic SSTs in ENSO variability: north tropical Atlantic SST and Atlantic Niño. Geophys. Res. Lett. 40, 4012–4017. https://doi.org/10.1002/grl.50729.

Hansen, J., Sato, M., Kharecha, P., von Schuckmann, K., 2011. Earth's energy imbalance and implications. Atmos. Chem. Phys. 11, 13421–13449. https://doi.org/10.5194/acp-11-13421-2011.

Harzallah, A., Sadourny, R., 1995. Internal versus SST-forced atmospheric variability as simulated by an atmospheric general circulation model. J. Clim. 8, 474–495. https://doi.org/10.1175/1520-0442(1995)008<0474:IVSFAV>2.0.CO;2.

Hoesly, R.M., Smith, S.J., Feng, L., Klimont, Z., Janssens-Maenhout, G., Pitkanen, T., Seibert, J.J., Vu, L., Andres, R.J., Bolt, R.M., Bond, T.C., Dawidowski, L., Kholod, N., Kurokawa, J., Li, M., Liu, L., Lu, Z., Moura, M.C.P., O'Rourke, P.R., Zhang, Q., 2018. Historical (1750–2014) anthropogenic emissions of reactive gases and aerosols from the community emissions data system (CEDS). Geosci. Model Dev. 11, 369–408. https://doi.org/10.5194/gmd-11-369-2018.

Hu, K., Huang, G., Huang, R., 2011. The impact of tropical Indian Ocean variability on summer surface air temperature in China. J. Clim. 24, 5365–5377. https://doi.org/10.1175/2011JCLI4152.1.

Hu, Z.-Z., 1997. Interdecadal variability of summer climate over East Asia and its association with 500 hPa height and global sea surface temperature. J. Geophys. Res. 102, 19403–19412. https://doi.org/10.1029/97JD01052.

IPCC, 2021. Climate Change 2021: The Physical Science Basis. Contribution of Working Group I to the Sixth Assessment Report of the Intergovernmental Panel on Climate Change [Masson-Delmotte, V., P. Zhai, A. Pirani, S.L. Connors, C. Péan, S. Berger, N. Caud, Y. Chen, L. Goldfarb, M.I. Gomis, *M. Huang*, K. Leitzell, E. Lonnoy, J.B.R. Matthews, T.K. Maycock, T. Waterfield, O. Yelekçi, R. Yu, and B. Zhou (eds.)]. Cambridge University Press, Cambridge, United Kingdom and New York, NY, USA, In press. https://doi.org/10.1017/9781009157896.

Jasaitis, D., Vasiliauskienė, V., Chadyšienė, R., Pečiulienė, M., 2016. Surface ozone concentration and its relationship with UV radiation. Meteorological Parameters and Radon on the Eastern Coast of the Baltic Sea, Atmosphere 7, 27. https://doi.org/10.3390/atmos7020027.

Jenkin, M.E., Clemitshaw, K.C., 2000. Ozone and other secondary photochemical pollutants: chemical processes governing their formation in the planetary boundary layer. Atmos. Environ. 34, 2499–2527. https://doi.org/10.1016/S1352-2310(99)00478-1.

Jiang, Z., Li, J., 2022. Impact of eastern and Central Pacific El Niño on lower tropospheric ozone in China. Atmos. Chem. Phys. 22, 7273–7285. https://doi.org/10.5194/acp-22-7273-2022.

Jiang, Z., Yang, H., Liu, Z., Wu, Y., Wen, N., 2014. Assessing the influence of regional SST modes on the winter temperature in China: the effect of tropical Pacific and Atlantic. J. Clim. 27, 868–879. https://doi.org/10.1175/JCLI-D-12-00847.1.

Kampa, M., Castanas, E., 2008. Human health effects of air pollution. Environ. Pollut. 151, 362–367. https://doi.org/10.1016/j.envpol.2007.06.012.

Kleinman, L.I., 2005. The dependence of tropospheric ozone production rate on ozone precursors. Atmos. Environ. 39, 575–586. https://doi.org/10.1016/j.atmosenv.2004.08.047.

Lamarque, J.-F., Emmons, L.K., Hess, P.G., Kinnison, D.E., Tilmes, S., Vitt, F., Heald, C.L., Holland, E.A., Lauritzen, P.H., Neu, J., Orlando, J.J., Rasch, P.J., Tyndall, G.K., 2012. CAM-chem: description and evaluation of interactive atmospheric chemistry in the community earth system model. Geosci. Model Dev. 5, 369–411. https://doi.org/10.5194/gmd-5- 369-2012.

Li, H., Yang, Y., Jin, J., Wang, H., Li, K., Wang, P., Liao, H., 2023a. Climate-driven deterioration of future ozone pollution in Asia predicted by machine learning with multi-source data. Atmos. Chem. Phys. 23, 1131–1145. https://doi.org/10.5194/acp-23-1131-2023.

Li, M., Yang, Y., Wang, H., Li, H., Wang, P., Liao, H., 2023c. Summertime ozone pollution in China affected by stratospheric quasi-biennial oscillation. Atmos. Chem. Phys. 23, 1533–1544. https://doi.org/10.5194/acp-23-1533-2023.

Li, P., Yang, Y., Wang, H., Li, S., Li, K., Wang, P., Li, B., Liao, H., 2023b. Source attribution of near-surface ozone trends in the United States during 1995–2019. Atmos. Chem. Phys. 23, 5403–5417. https://doi.org/10.5194/acp-23-5403-2023.

Li, X., Liu, J., Mauzerall, D.L., Emmons, L.K., Walters, S., Horowitz, L.W., Tao, S., 2014. Effects of trans-Eurasian transport of air pollutants on surface ozone concentrations over Western China. J. Geophys. Res.-Atmos. 119, 12338–12354. https://doi.org/10.1002/2014JD021936.

Lin, M., Horowitz, L.W., Oltmans, S.J., Fiore, A.M., Fan, S., 2014. Tropospheric ozone trends at Mauna Loa observatory tied to decadal climate variability. Nat. Geosci. 7, 136–143. https://doi.org/10.1038/ngeo2066.

Liu, J., Mauzerall, D.L., Horowitz, L.W., 2005. Analysis of seasonal and interannual variability in transpacific transport. J. Geophys. Res. 110, D04302. https://doi.org/10.1029/2004JD005207.

Liu, S., Duan, A., 2018. Impacts of the global sea surface temperature anomaly on the evolution of circulation and precipitation in East Asia on a quasi-quadrennial cycle. Clim. Dyn. 51, 4077–4094. https://doi.org/10.1007/s00382-017-3663-4.

Lucas, R.M., Yazar, S., Young, A.R., Norval, M., De Gruijl, F.R., Takizawa, Y., Rhodes, L. E., Sinclair, C.A., Neale, R.E., 2019. Human health in relation to exposure to solar ultraviolet radiation under changing stratospheric ozone and climate. Photochem. Photobiol. Sci. 18, 641–680. https://doi.org/10.1039/c8pp90060d.

Manisalidis, I., Stavropoulou, E., Stavropoulos, A., Bezirtzoglou, E., 2020. Environmental and health impacts of air pollution: a review. Front. Public Health 8, 14. https://doi.org/10.3389/fpubh.2020.00014.

Meinshausen, M., Nicholls, Z.R.J., Lewis, J., Gidden, M.J., Vogel, E., Freund, M., Beyerle, U., Gessner, C., Nauels, A., Bauer, N., Canadell, J.G., Daniel, J.S., John, A., Krummel, P.B., Luderer, G., Meinshausen, N., Montzka, S.A., Rayner, P.J., Reimann, S., Smith, S.J., van den Berg, M., Velders, G.J.M., Vollmer, M.K., Wang, R. H.J., 2020. The shared socio-economic pathway (SSP) greenhouse gas concentrations and their extensions to 2500. Geosci. Model Dev. 13, 3571–3605. https://doi.org/10.5194/gmd-13-3571-2020.

Meleux, F., Solmon, F., Giorgi, F., 2007. Increase in summer European ozone amounts due to climate change. Atmos. Environ. 41, 7577–7587. https://doi.org/10.1016/j.atmosenv.2007.05.048.

Monks, P.S., Granier, C., Fuzzi, S., Stohl, A., Williams, M.L., Akimoto, H., Amann, M., Baklanov, A., Baltensperger, U., Bey, I., Blake, N., Blake, R.S., Carslaw, K., Cooper, O.R., Dentener, F., Fowler, D., Fragkou, E., Frost, G.J., Generoso, S., Ginoux, P., Grewe, V., Guenther, A., Hansson, H.C., Henne, S., Hjorth, J., Hofzumahaus, A., Huntrieser, H., Isaksen, I.S.A., Jenkin, M.E., Kaiser, J., Kanakidou, M., Klimont, Z., Kulmala, M., Laj, P., Lawrence, M.G., Lee, J.D., Liousse, C., Maione, M., McFiggans, G., Metzger, A., Mieville, A., Moussiopoulos, N., Orlando, J.J., O'Dowd, C.D., Palmer, P.I., Parrish, D.D., Petzold, A., Platt, U., Pöschl, U., Prévôt, A.S.H., Reeves, C.E., Reimann, S., Rudich, Y., Sellegri, K., Steinbrecher, R., Simpson, D., ten Brink, H., Theloke, J., van der Werf, G.R., Vautard, R., Vestreng, V., Vlachokostas, Ch., von Glasow, R., 2009. Atmospheric composition change – global and regional air quality. Atmos. Environ. 43, 5268–5350. https://doi.org/10.1016/j.atmosenv.2009.08.021.

Monks, P.S., Archibald, A.T., Colette, A., Cooper, O., Coyle, M., Derwent, R., Fowler, D., Granier, C., Law, K.S., Mills, G.E., Stevenson, D.S., Tarasova, O., Thouret, V., von Schneidemesser, E., Sommariva, R., Wild, O., Williams, M.L., 2015. Tropospheric ozone and its precursors from the urban to the global scale from air quality to short-lived climate forcer. Atmos. Chem. Phys. 15, 8889–8973. https://doi.org/10.5194/acp-15-8889-2015.

Oltmans, S.J., Levy, H., 1994. Surface ozone measurements from a global network. Atmos. Environ. 28, 9–24. https://doi.org/10.1016/1352-2310(94)90019-1.

Phalitnonkiat, P., Hess, P.G.M., Grigoriu, M.D., Samorodnitsky, G., Sun, W., Beaudry, E., Tilmes, S., Deushi, M., Josse, B., Plummer, D., Sudo, K., 2018. Extremal dependence between temperature and ozone over the continental US. Atmos. Chem. Phys. 18, 11927–11948. https://doi.org/10.5194/acp-18-11927-2018.

Pillai, S., Oresajo, C., Hayward, J., 2005. Ultraviolet radiation and skin aging: roles of reactive oxygen species, inflammation and protease activation, and strategies for prevention of inflammation-induced matrix degradation – a review. Int. J. Cosmet. Sci. 27, 17–34. https://doi.org/10.1111/j.1467-2494.2004.00241.x.

Pusede, S.E., Steiner, A.L., Cohen, R.C., 2015. Temperature and recent trends in the chemistry of continental surface ozone. Chem. Rev. 115, 3898–3918. https://doi.org/10.1021/cr5006815.

Rasmussen, D.J., Fiore, A.M., Naik, V., Horowitz, L.W., McGinnis, S.J., Schultz, M.G., 2012. Surface ozone-temperature relationships in the eastern US: a monthly climatology for evaluating chemistry-climate models. Atmos. Environ. 47, 142–153. https://doi.org/10.1016/j.atmosenv.2011.11.021.

Rong, X., Zhang, R., Li, T., 2010. Impacts of Atlantic Sea surface temperature anomalies on indo-east Asian summer monsoon-ENSO relationship. Chin. Sci. Bull. 55, 2458–2468. https://doi.org/10.1007/s11434-010-3098-3.

Schleussner, C.-F., Rogelj, J., Schaeffer, M., Lissner, T., Licker, R., Fischer, E.M., Knutti, R., Levermann, A., Frieler, K., Hare, W., 2016. Science and policy characteristics of the Paris agreement temperature goal. Nat. Clim. Chang. 6, 827–835. https://doi.org/10.1038/nclimate3096.

Schnell, R.C., Oltmans, S.J., Neely, R.R., Endres, M.S., Molenar, J.V., White, A.B., 2009. Rapid photochemical production of ozone at high concentrations in a rural site during winter. Nat. Geosci. 2, 120–122. https://doi.org/10.1038/ngeo415.

Seager, R., Henderson, N., 2016. On the role of Tropical Ocean forcing of the persistent north American west coast ridge of winter 2013/14. J. Clim. 29, 8027–8049. https://doi.org/10.1175/JCLI-D-16-0145.1.

Shen, L., Mickley, L.J., 2017. Effects of El Niño on summertime ozone air quality in the eastern United States. Geophys. Res. Lett. 44, 12543–12550. https://doi.org/10.1002/2017GL076150.

Sillman, S., Samson, P.J., 1995. Impact of temperature on oxidant photochemistry in urban, polluted rural and remote environments. J. Geophys. Res. 100, 11497. https://doi.org/10.1029/94JD02146.

Su, B., Huang, J., Mondal, S.K., Zhai, J., Wang, Y., Wen, S., Gao, M., Lv, Y., Jiang, S., Jiang, T., Li, A., 2021. Insight from CMIP6 SSP-RCP scenarios for future drought characteristics in China. Atmos. Res. 250, 105375 https://doi.org/10.1016/j.atmosres.2020.105375.

Sun, B., Li, H., Zhou, B., 2019. Interdecadal variation of Indian Ocean basin mode and the impact on Asian summer climate. Geophys. Res. Lett. 46, 12388–12397. https://doi.org/10.1029/2019GL085019.

Tai, A.P.K., Martin, M.V., Heald, C.L., 2014. Threat to future global food security from climate change and ozone air pollution. Nat. Clim. Chang. 4, 817–821. https://doi.org/10.1038/nclimate2317.

Tilmes, S., Lamarque, J.-F., Emmons, L.K., Kinnison, D.E., Ma, P.-L., Liu, X., Ghan, S., Bardeen, C., Arnold, S., Deeter, M., Vitt, F., Ryerson, T., Elkins, J.W., Moore, F., Spackman, J.R., Val Martin, M., 2015. Description and evaluation of tropospheric chemistry and aerosols in the Community Earth System Model (CESM1.2). Geosci. Model Dev. 8, 1395–1426. https://doi.org/10.5194/gmd-8-1395-2015.

Tilmes, S., Lamarque, J.-F., Emmons, L.K., Kinnison, D.E., Marsh, D., Garcia, R.R., Smith, A.K., Neely, R.R., Conley, A., Vitt, F., Val Martin, M., Tanimoto, H., Simpson, I., Blake, D.R., Blake, N., 2016. Representation of the community earth system model (CESM1) CAM4-chem within the chemistry-climate model initiative (CCMI). Geosci. Model Dev. 9, 1853–1890. https://doi.org/10.5194/gmd-9-1853-2016.

Trenberth, K.E., Fasullo, J.T., Balmaseda, M.A., 2014. Earth's energy imbalance. J. Clim. 27, 3129–3144. https://doi.org/10.1175/JCLI-D-13-00294.1.

Ueda, H., Kamae, Y., Hayasaki, M., Kitoh, A., Watanabe, S., Miki, Y., Kumai, A., 2015. Combined effects of recent Pacific cooling and Indian Ocean warming on the asian monsoon. Nat. Commun. 6, 8854. https://doi.org/10.1038/ncomms9854.

Val Martin, M., Heald, C.L., Lamarque, J.-F., Tilmes, S., Emmons, L.K., Schichtel, B.A., 2015. How emissions, climate, and land use change will impact mid-century air quality over the United States: a focus on effects at national parks. Atmos. Chem. Phys. 15, 2805–2823. https://doi.org/10.5194/acp-15-2805-2015.

van Marle, M.J.E., Kloster, S., Magi, B.I., Marlon, J.R., Daniau, A.-L., Field, R.D., Arneth, A., Forrest, M., Hantson, S., Kehrwald, N.M., Knorr, W., Lasslop, G., Li, F., Mangeon, S., Yue, C., Kaiser, J.W., van der Werf, G.R., 2017. Historic global biomass burning emissions for CMIP6 (BB4CMIP) based on merging satellite observations with proxies and fire models (1750–2015). Geosci. Model Dev. 10, 3329–3357. https://doi.org/10.5194/gmd-10-3329-2017.

Vecchi, G.A., Soden, B.J., 2007. Effect of remote sea surface temperature change on tropical cyclone potential intensity. Nature 450, 1066–1070. https://doi.org/10.1038/nature06423.

Wang, P., Yang, Y., Li, H., Chen, L., Dang, R., Xue, D., Li, B., Tang, J., Leung, L.R., Liao, H., 2022. North China plain as a hot spot of ozone pollution exacerbated by extreme high temperatures. Atmos. Chem. Phys. 22, 4705–4719. https://doi.org/10.5194/acp-22-4705-2022.

Wang, T., Wong, H.L.A., Tang, J., Ding, A., Wu, W.S., Zhang, X.C., 2006. On the origin of surface ozone and reactive nitrogen observed at a remote mountain site in the northeastern Qinghai-Tibetan plateau, western China. J. Geophys. Res. 111, D08303. https://doi.org/10.1029/2005JD006527.

Wijffels, S., Roemmich, D., Monselesan, D., Church, J., Gilson, J., 2016. Ocean temperatures chronicle the ongoing warming of earth. Nat. Clim. Chang. 6, 116–118. https://doi.org/10.1038/nclimate2924.

Xie, M., Liao, J., Wang, T., Zhu, K., Zhuang, B., Han, Y., Li, M., Li, S., 2016. Modeling of the anthropogenic heat flux and its effect on regional meteorology and air quality over the Yangtze River Delta region, China. Atmos. Chem. Phys. 16, 6071–6089. https://doi.org/10.5194/acp-16-6071-2016.

Xie, M., Shu, L., Wang, T.J., Liu, Q., Gao, D., Li, S., Zhuang, B.L., Han, Y., Li, M.M., Chen, P.L., 2017. Natural emissions under future climate condition and their effects on surface ozone in the Yangtze River Delta region, China. Atmos. Environ. 150, 162–180. https://doi.org/10.1016/j.atmosenv.2016.11.053.

Yang, Y., Liao, H., Li, J., 2014. Impacts of the east Asian summer monsoon on interannual variations of summertime surface-layer ozone concentrations over China. Atmos. Chem. Phys. 14, 6867–6879. https://doi.org/10.5194/acp-14-6867-2014.

Yang, Y., Li, M., Wang, H., Li, H., Wang, P., Li, K., Gao, M., Liao, H., 2022. ENSO modulation of summertime tropospheric ozone over China. Environ. Res. Lett. 17, 034020 https://doi.org/10.1088/1748-9326/ac54cd.

Yi, K., Liu, J., Ban-Weiss, G., Zhang, J., Tao, W., Cheng, Y., Tao, S., 2017. Response of the global surface ozone distribution to northern Hemisphere Sea surface temperature changes: implications for long-range transport. Atmos. Chem. Phys. 17, 8771–8788. https://doi.org/10.5194/acp-17-8771-2017.

Yin, Z., Cao, B., Wang, H., 2019. Dominant patterns of summer ozone pollution in eastern China and associated atmospheric circulations. Atmos. Chem. Phys. 19, 13933–13943. https://doi.org/10.5194/acp-19-13933-2019.

Yoo, S.-H., Yang, S., Ho, C.-H., 2006. Variability of the Indian Ocean Sea surface temperature and its impacts on Asian-Australian monsoon climate. J. Geophys. Res. 111, D03108. https://doi.org/10.1029/2005JD006001.

Young, P.J., Archibald, A.T., Bowman, K.W., Lamarque, J.-F., Naik, V., Stevenson, D.S., Tilmes, S., Voulgarakis, A., Wild, O., Bergmann, D., Cameron-Smith, P., Cionni, I., Collins, W.J., Dalsøren, S.B., Doherty, R.M., Eyring, V., Faluvegi, G., Horowitz, L.W., Josse, B., Lee, Y.H., MacKenzie, I.A., Nagashima, T., Plummer, D.A., Righi, M., Rumbold, S.T., Skeie, R.B., Shindell, D.T., Strode, S.A., Sudo, K., Szopa, S., Zeng, G., 2013. Pre-industrial to end 21st century projections of tropospheric ozone from the Atmospheric Chemistry and Climate Model Intercomparison Project (ACCMIP). Atmos. Chem. Phys. 13, 2063–2090. https://doi.org/10.5194/acp-13-2063-2013.

Yue, X., Unger, N., Harper, K., Xia, X., Liao, H., Zhu, T., Xiao, J., Feng, Z., Li, J., 2017. Ozone and haze pollution weakens net primary productivity in China. Atmos. Chem. Phys. 17, 6073–6089. https://doi.org/10.5194/acp-17-6073-2017.

Zanis, P., Akritidis, D., Turnock, S., Naik, V., Szopa, S., Georgoulias, A.K., Bauer, S.E., Deushi, M., Horowitz, L.W., Keeble, J., Le Sager, P., O'Connor, F.M., Oshima, N., Tsigaridis, K., van Noije, T., 2022. Climate change penalty and benefit on surface ozone: a global perspective based on CMIP6 earth system models. Environ. Res. Lett. 17, 024014 https://doi.org/10.1088/1748-9326/ac4a34.

Zhang, P., Duan, A., Hu, J., 2022. Combined effect of the tropical Indian Ocean and tropical North Atlantic Sea surface temperature anomaly on the Tibetan plateau precipitation anomaly in late summer. J. Clim. 35, 7499–7518. https://doi.org/10.1175/JCLI-D-21-0990.1.

Zhou, Y., Yang, Y., Wang, H., Wang, J., Li, M., Li, H., Wang, P., Zhu, J., Li, K., Liao, H., 2022. Summer ozone pollution in China affected by the intensity of Asian monsoon systems. Sci. Total Environ. 849, 157785 https://doi.org/10.1016/j.scitotenv.2022.157785.